Direct Investigation of Intracellular Presence of Gold Nanoparticles *via* Photothermal Heterodyne Imaging

Cécile Leduc,[⊥,†] Jin-Mi Jung,[⊥,‡] Randy R. Carney,[‡,§] Francesco Stellacci,[‡,§,*] and Brahim Lounis[†,*]

[†]LP2N Institut d'Optique, Université de Bordeaux, CNRS & IOGS-Bordeaux, Talence F-33405, France, [‡]Department of Materials Science and Engineering, Massachusetts Institute of Technology, Cambridge, Massachusetts 02139, United States , and [§]Institute of Materials, École polytechnique fédérale de Lausanne, Lausanne, 1015, Switzerland. [⊥]These authors contributed equally to this work.

ABSTRACT Nanotechnology as well as advanced microscopy can play a fundamental role in understanding biological mechanisms. Here we present a study that combines a new type of nanomaterial with a new type of microscopy and highlights the potential for gathering novel information about cell membrane penetration and cytosol local viscosity. On the material side, we used gold nanoparticles that have an ordered stripe-like arrangement of domains. These "striped" nanoparticles are able to penetrate cell membranes directly without porating them. On the microscopy side, we used photothermal heterodyne imaging which allows detection of individual nanometer-sized gold particles in complex media. We showed that we can probe cytosolic presence as well as dynamics of these nanoparticles even at very low concentrations. We used the fluctuations of the photothermal signal from particles diffusing in the detection volume to estimate local cytosol viscosity which is about 20 times larger than that of water. This work opens new perspectives for mapping local diffusion properties of nano-objects inside living cells.

KEYWORDS: gold nanoparticle · cell penetration · photothermal imaging · cytosol viscosity · self-assembled monolayer

There is a rapidly growing interest in using nanoparticles (NPs) as key tools in medicine either for drug delivery or as novel imaging contrast agent, or local probes/sensors.[1−3] Among the nanoscale synthetic materials "striped" nanoparticles are an interesting class of particles able to penetrate cell membranes without porating them.[4] These are gold nanoparticles coated with a self-assembled monolayer composed of a mixture of dislike thiolated molecules (ligands); it has been established that stripe-like domains of alternating composition only a few molecules thick (see also cartoon in Figure 1)[4−7] spontaneously form due to the interplay between the enthalpy of phase-separation and the conformational entropy gain of longer ligands surrounded by shorter ones.[8] When these stripes consist of alternating hydrophobic/hydrophilic domains unique properties arise;[5−7] for example, a structural component to the interfacial energy can be experimentally observed.[9] In a recent study, we have shown that MUS/OT AuNPs, particles coated with a mixture of 11-mercapto-undecane sulfonic acid (MUS) and 1-octanethiol (OT), show stripe-like domains (Figure 1) and pass cell membranes without porating them in an energy independent manner besides being endocytosed.[4] On the contrary, particles coated solely with MUS (all-MUS AuNPs) with no structure on their ligand shells penetrate the cell only *via* endocytotic process.

The original studies were based on either transmission electron microscopy (TEM) or fluorescence labeling. However, TEM studies are extremely time-consuming, invasive, and do not allow dynamics measurements. Therefore it is unreasonable to base future large systematic studies on such a technique. Fluorescence studies suffer from limitations related first to luminescence quenching by the metal particles and photobleaching. This makes it difficult to extract any quantitative information on the particle concentration and dispersion from the fluorescence intensity. Second, because of the fluorescent label detachment, the access to the long time scale (days) behavior of the particles is limited if not impossible.[10] Third, the influence of the fluorophore in cell penetration although weak cannot be completely neglected and needs to be ruled out through laborious TEM studies. Finally, in order to have measurable fluorescence signals, high incubation particle concentrations (∼100 nM) and times (∼3 h at 37 °C) are necessary. Since endocytic pathways of uptake take around 1 h,[14] previous studies at 37 °C could not distinguish between particles that had directly penetrated cell membranes and particles that had escaped endosomes.[4]

To overcome these limitations, we used the extremely sensitive photothermal heterodyne imaging technique (PHI) which

* Address correspondence to francesco.stellacci@epfl.ch, blounis@u-bordeaux1.fr.

Received for review September 7, 2010 and accepted March 9, 2011.

Published online March 09, 2011
10.1021/nn1023285

© 2011 American Chemical Society

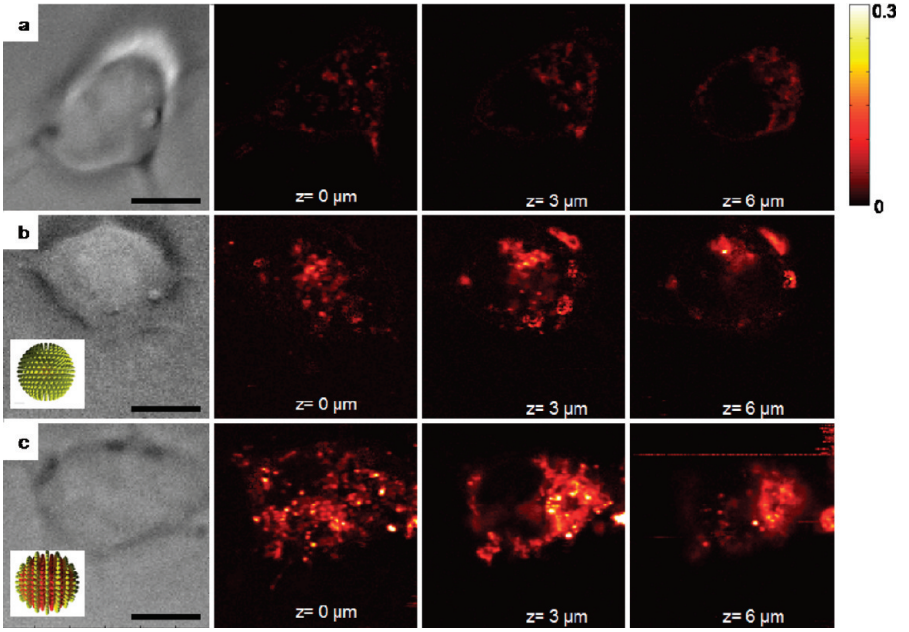

Figure 1. Bright field images (far left) and *z*-stack of photothermal images (right) of (a) typical nonincubated cell used as control, (b) all-MUS AuNPs incubated cell, and (c) MUS/OT AuNPs incubated cell. Cells were incubated with 10 nM AuNPs for 1 h at 37 °C. Bar, 10 μm. Insets in panels b and c represent cartoons of a uniformly coated all-MUS AuNP and a striped MUS/OT AuNP, respectively.

allows direct detection of individual nanometer-sized gold NPs.[11] We studied the internalization of MUS/OT NPs without any fluorescence labeling in live cells in a quantitative manner and were able to probe their dynamics during arbitrary long time scales. Contrary to unstructured particles (all-MUS AuNPs), "striped" MUS/OT NPs incubated both at 37 °C and at 4 °C were detected even at extremely low incubation concentrations (concentrations well below those used in fluorescence microscopy[4]) and shorter incubation times. Thus, PHI allowed us to substantially better elucidate the cellular behavior of cell-penetrating nanoparticles. Finally, using the PHI signal fluctuations due to the NPs movement through the detection volume we could estimate the local viscosity of the cytosol.

RESULT AND DISCUSSION

The PHI technique has been developed for the detection of small absorbing NPs such as gold nanospheres when excited close to their plasmon resonance. The experimental setup is described elsewhere.[13] In brief, a time-modulated green heating beam (CW, wavelength 532 nm, modulation frequency of 10 kHz) is superimposed with a nonresonant probe beam. When an absorbing nano-object is in the detection volume of the two highly focused beams, all the absorbed green laser energy is converted to heat that induces a time-modulated variation of the refractive index around this nano-object. The interaction of the probe beam with this index profile produces a scattered field with sidebands at the modulation frequency. The scattered field is then detected in the forward direction through its beatnote with the transmitted probe field.

Because the plasmon resonance of extremely small Au NPs (diameter of NPs used in these experiments <5 nm) is broad and not well pronounced, we modified our PHI setup and used a CW Nd:Yag laser (wavelength 1064 nm) as well as a InGaS photodiode to probe the photothermal effect. The detection volume is defined by the spatial resolution of the PHI method and is simply given by the product of the probe and heating beam profiles at the objective focus.[13] In our setup, the detection volume can be approximated by the green-beam intensity profile because the probe beam profile is significantly larger than the green one. Using a heating beam power of ~2 mW and a probe power of ~10 mW, single 4 nm nanoparticles can be imaged with a reasonable signal-to-noise ratio (~10) with an integration time of 5 ms. For quantitative comparison between the results obtained in this work, these experimental parameters were kept the same during all the experiments.

Owing to its unsurpassed sensitivity in detecting absorbing objects, PHI technique images unlabeled mitochondria in live cells,[15] a well-known light absorbing cellular organelle. Figure 1a shows a typical PHI images *z*-stack of mouse dendritic cells (DC 2.4) which display such a weak background generated from mitochondria (the $z = 0$ plane corresponds to the glass surface).

When incubated with all-MUS AuNPs for 1 h at 37 °C, photothermal images of the DC 2.4 cells (Figure 1b) showed an overall relatively low intensity signal which is comparable to that of mitochondria (Figure 1a). A

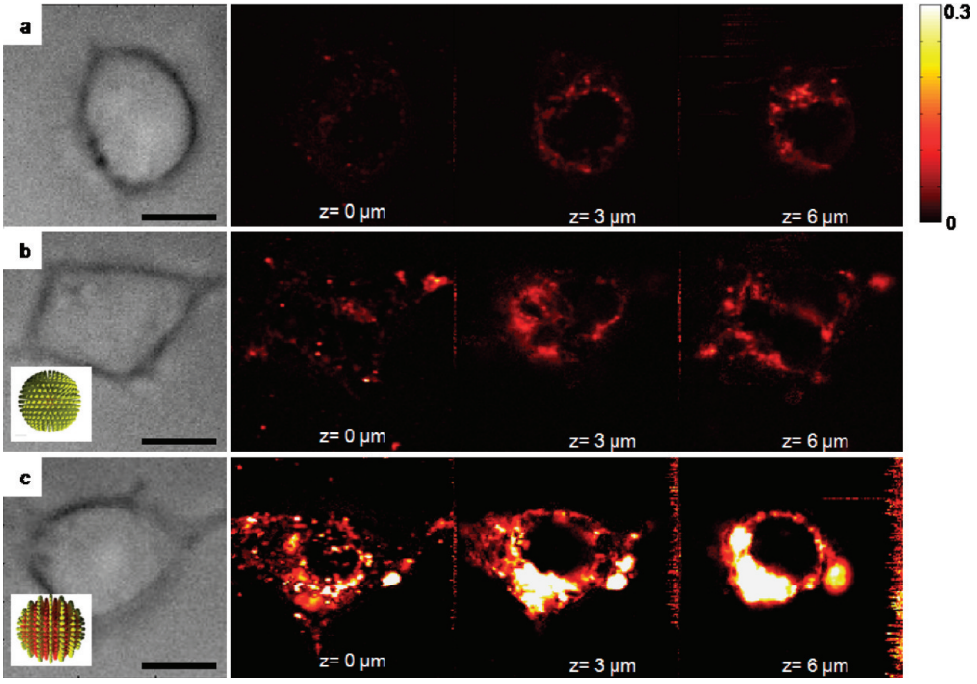

Figure 2. Bright field images (far left) and *z*-stack of photothermal images (right) of (a) typical nonincubated cell used as control, (b) all-MUS AuNPs incubated cell, and (c) MUS/OT AuNPs incubated cell. Cells were incubated with 10 nM AuNPs for 3 h at 4 °C. Bar, 10 μm. Note that PHI signal bar is the same as in Figure 1. Insets in panels b and c represent cartoons of a uniformly coated all-MUS AuNP and a striped MUS/OT AuNP, respectively.

few bright spots localized in the cytosol, are also observed and could be attributed to either particles trapped in endosomal aggregates or local particle precipitations in the cytosol. PHI images of cells incubated with MUS/OT AuNPs in the same conditions showed a higher continuous signal that we attribute to NPs with fast diffusion in the cytosol, together with a larger number of bright spots (Figure 1c). In the middle plane of the z-stack, the dark region corresponds to the cell nucleus indicating that the Au NPs do not go through the nucleus membrane as previously observed.[4] When incubated with MUS/OT AuNPs for 1 h at 37°, cells displayed an average photothermal signal three time higher than when incubated with all-MUS NPs (averaged signal per cell of 0.09 $\pm$ 0.03 au, mean $\pm$SD over 6 cells, compared to 0.026 $\pm$ 0.013 au, over 6 cells, respectively). Because internalization *via* endocytosis is expected to be similar for all-MUS and MUS/OT AuNPs and in any case happens at longer time scales (3 h compared to the 1 h incubation time used here), the observation of a larger number of bright spots with MUS/OT NPs suggests that these spots rather stem from local cytosolic particle aggregates. These observations indicate direct cell membrane penetration of MUS/OT AuNPs. Note that the incubation concentration of NPs used for these images was 10 nM already 10 times lower than the minimal concentration that could be used in fluorescence studies.[4] We also checked the cell integrity after PHI imaging with bright field illumination; no morphological changes were observed (see Supporting Information).

To exclude any internalization process involving endocytosis and further confirm direct cell membrane penetration, we performed experiments on cells incubated with a dilute particle solutions (10 nM) at 4 °C for 3 h. Indeed, there is no ATP/ADP conversion at this temperature and therefore no energy driven process such as endocytosis. As shown in Figure 2, PHI images of a control cell (in the absence of any Au NPs) and an all-MUS Au NPs-incubated cell present similar signal levels indicating that internalization is limited. On the contrary cells incubated with MUS/OT NPs display large PHI signals (see also Supporting Information, Figures S5 and S6). These results confirm that striped particles can pass cell membrane and also are present in the cytosol. Because they were obtained with non-fluorescently labeled particles, these results also point out a minimal effect of fluorophores on cell membrane penetration as pointed out in reference 4. One can note that the bright regions are not found on the boundary of the cell, they are only in its central parts excluding the nucleus. Therefore, our observation suggests that most particles converge into free cytosol space (far from the actin-rich edges[16] after penetrating). These results are in agreement with the TEM images previously published, where particles in the cytosol were found to be inhomogeneously distributed.[4]

To further substantiate this finding, we investigated the minimum incubation concentrations that could be used to detect cytosolic particles in a cell, a relevant parameter for many studies where it is most desirable to minimize the perturbation to a biological system. To

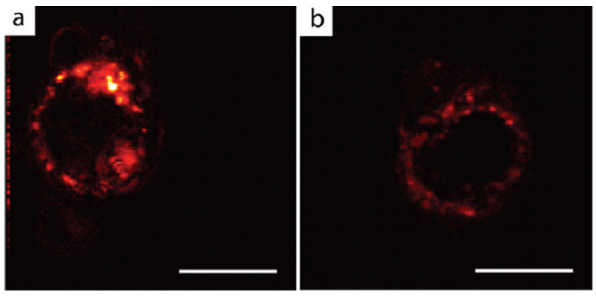

Figure 3. (a) PHI image of a DC cell incubated for 3 h at 4 °C with 1 nM MUS/OT AuNP particle solution. (b) PHI image of a control cell. The scale bar is 10 μm. The PHI signal bar is the same as in Figure 1.

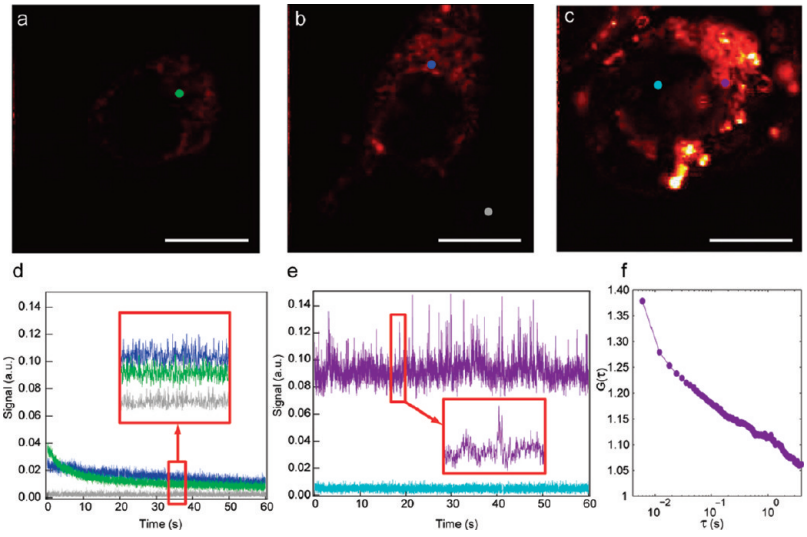

Figure 4. PHI images of a (a) control cell (no particles), (b) all-MUS AuNP (100 nM) incubated cell, and (c) MUS/OT AuNP (50 nM) incubated cell for 1 h at 37 °C. Bars, 10 μm. (d) Time traces at different positions of the cells and the surface: the green curve was recorded on the cell in panel a, the blue curve on the cell in panel b, the gray curve was recorded outside of the cell in panel b. (e) Time trace records of the cell in panel c: the sky blue curve inside the cell nucleus and the purple curve in the bright region of the cell in panel c. (f) Correlation function of the purple signal time trace. For the sake of comparison, the PHI signal bar in panels a−c is the same as in Figure 1.

avoid endocytosis, the incubations were performed at 4 °C. Cells were incubated for 3 h with particle solutions of 100, 50, 10, 1, and 0.1 nM concentration. For relatively high concentrations of MUS/OT particles (from 100 to 10 nM) very bright signals were observed. The lowest incubation concentration at which we could still detect MUS/OT NPs inside cells was 1 nM. Figure 3 shows a PHI image of a cell incubated at this concentration together with a control cell. In this case, the average PHI intensity per incubated cell was two times larger than that of control cells (6 cells analyzed). Below such concentration, only photothermal signal from mitochondria is observed (see Supporting Information). We clearly show here that by using the PHI method we improved the sensitivity of internalized NPs detection by 2 orders of magnitude in the incubation concentration in comparison with previous measurements based on fluorescence (see Supporting Information, Figure S4).[4]

A remaining question concerns the dynamics of penetrating particles inside the cell cytosol. To address this point, we used the time fluctuations of the photothermal signal recorded with laser-beams focused at fixed positions inside the cell. Figure 4d shows examples of signal time traces acquired on a control cell (not-incubated with AuNPs, imaged in Figure 4a) and cells incubated with the two different particle types, all-MUS AuNPs (figure 4b) and MUS/OT AuNPs (figure 4c). In the control and all-MUS conditions, the PHI traces present a typical time decay coming from the bleaching of the mitochondria signal.[15] The absence of signal bursts in the all-MUS AuNPs-incubated confirms the fact that the NPs do not penetrate the cell membranes. When we traced the signal at a bright region of a PHI image of MUS/OT AuNPs-incubated cell, we observed bursts, signal fluctuations which are larger than the noise and no signal bleaching. We consistently observed the same signal fluctuations in many images from MUS/OT incubated cells independently of the incubation concentrations (12 cells incubated at 37 °C).

Using the time fluctuations of the signal one can set an upper limit for the cytosolic viscosity. We used the photothermal absorption correlation spectroscopy[17] to measure the average transit time of the particles in the fixed detection volume which is here given by the focal volume of the heating beam.[13] Figure 4f displays the photothermal intensity correlation curve of the time trace recorded in the bright region of Figure 4c. The lack of a plateau at short times in the curve is an indication that the average particle diffusion time is shorter than the signal integration time (5 ms). Assuming a free diffusion of particles in the cytosol, one can obtain a maximum value of $\sim 2 \times 10^{-2}$ Pa·s for the cytosolic viscosity, about 20 times larger than that of water. This value falls in the range of previous global or local viscosity measurements based on various fluorescence techniques (from 2×10^{-3} to 2×10^{-1} Pa·s).[18−23]

CONCLUSION

We have shown that PHI is a powerful technique to visualize gold particles inside living cell, especially at very low concentrations. This has been used to prove that striped nanoparticles are present in the cytosol and can directly penetrate cell-membranes. The combination of PHI and striped nanoparticles was used to estimate the local cell viscosity.

We believe that the use of cell-penetrating nanoprobes with absorption resonances tailored in the near-infrared (gold rods, core/shell particles) will substantially improve the quality of the data acquired by reducing the background signal of mitochondria. This could be the start of a series of studies that elucidate cell/nanomaterials interactions as well as local cell viscosity properties.

MATERIALS AND METHODS

Nanoparticle Synthesis. The nanoparticles were prepared by a modified one-phase synthesis[12] in which a gold salt, $HAuCl_4$, was dissolved in ethanol followed by the addition of a solution of thiolated ligands (1:1 ligand/gold molar ratio). A strong reducing agent, sodium borohydride, was added dropwise, and the solution was stirred for 2 h, refrigerated overnight to precipitate, and washed over filter paper with ethanol, methanol, and acetone. For this system, the thiolated ligands were a 2:1 molar mixture of 11-mercapto-1-undecanesulfonate (MUS) and 1-octanethiol (OT), respectively, as determined *via* decomposition NMR studies of the type described previously. The nanoparticles were then dissolved in PBS buffer (pH 7.4) in order to make a stock solution with a concentration of 4 mg/mL. The all-MUS AuNPs were coated with a homogeneous (and hence unstructured) monolayer of MUS. The MUS/OT AuNPs were coated with a mixed (and striped[4,5]) monolayer composed of a 2:1 molar mixture of MUS and OT.

Cell Culture and Sample Preparation for PHI. Mouse dendritic cells (DC) clone, DC 2.4 were grown in RPMI 1640 medium supplemented with L-glutamin and 10% fetal bovine serum at 37 °C. The cells were plated on round glass coversilps (diameter 16 mm) at 0.5×10^5 cells per cm^2 that were previously placed in a 12 well cell culture microplate. After a 15−17 h incubation time with RPMI serum-containing medium, the medium was changed with fresh warm RPMI serum-free medium and the stock particle solution was added at a target concentration of 100 nM, 50 nM, 10 nM, 1 nM or 0.1 M. Cells were incubated with nanoparticles for 1 h at 37 °C (or 3 h for 4 °C experiment) and then washed with serum-free medium five times. Thereafter, the cell-coated coverslips were mounted onto a sample holder for PHI. A drop of colorless Ringer's buffer (155 mM NaCl, 5 mM KCl, 2 mM $CaCl_2$, 1 mM $MgCl_2 \cdot 6H_2O$, 2 mM $NaH_2PO_4 \cdot H_2O$, 10 mM HEPES, and 10 mM glucose) was added on the cell surface and another clean glass coverslip was placed and fixed onto the first one. We made sure the mounted sample was leak-free and that cells survived for several hours even after imaging performed at room temperature.

Acknowledgment. This work was supported by the Korea Research Foundation Grant funded by the Korean Government (MOEHRD, Basic Research Promotion Fund) (KRF-2008-357-00090) and by the Région Aquitaine, the Agence Nationale pour la Recherche (program PNANO and PCV), and the European Research Council (ERC Advanced Investigators Grant). We would like to acknowledge Laurent Cognet for helpful discussions.

Supporting Information Available: Additional PHI images, optical images, and fluorescence images for comparative study. This material is available free of charge *via* the Internet at http://pubs.acs.org.

REFERENCES AND NOTES

1. Borgdorff, A. J.; Choquet, D. Regulation of AMPA Receptor Lateral Movements. *Nature* **2002,** *417*, 649–653.
2. Anker., J. N.; Hall, W. P.; Lyandres, O.; Shah, N. C.; Zhao, J.; Van Duyne, R. P. Biosensing with Plasmonic Nanosensors. *Nat. Mater.* **2008,** *7*, 442–453.
3. Boisselier, E.; Astruc, D. Gold Nanoparticles in Nanomedicine: Preparations, Imaging, Diagnostics, Therapies and Toxicity. *Chem. Soc. Rev.* **2009,** *38*, 1759–1782.
4. Verma, A.; Uzun, O.; Hu, Y.; Hu, Y.; Han, H.-S.; Watson, N.; Chen, S.; Irvine, D. J.; Stellacci, F. Surface-Structure-Regulated Cell-Membrane Penetration by Monolayer-Protected Nanoparticles. *Nat. Mater.* **2008,** *7*, 588–595.
5. Jackson, A. M.; Myerson, J. W.; Stellacci, F. Spontaneous Assembly of Subnanometre-Ordered Domains in the Ligand Shell of Monolayer-Protected Nanoparticles. *Nat. Mater.* **2004,** *3*, 330–336.
6. Jackson, A. M.; Hu, Y.; Silva, P.; Stellacci, F. From Homoligand- to Mixed-Ligand- Monolayer-Protected Metal Nanoparticles: A Scanning Tunneling Microscopy Investigation. *J. Am. Chem. Soc.* **2006,** *128*, 11135–11149.
7. Uzun, O.; Hu, Y.; Verma, A.; Chen, S.; Centrone, A.; Stellacci, F. Water Soluble Amphiphilic Gold Nanoparticles with Structured Ligand Shells. *J. Chem Soc., Chem. Commun.* **2008,** *2*, 196–198.
8. Singh, C.; Ghorai, P. K.; Horsch, M. A.; Jackson, A. M.; Larson, R. G.; Stellacci, F.; Glotzer, S. C. Entropy-Mediated Patterning of Surfactant-Coated Nanoparticles and Surfaces. *Phys. Rev. Lett.* **2007,** *99*, 226106.
9. Kuna, J. J.; Voïtchovsky, K.; Singh, C.; Jiang, H.; Mwenifumbo, S.; Ghorai, P. K.; Stevens, M. M.; Glotzer, S. C.; Stellacci, F. The Effect of Nanometre-Scale Structure on Interfacial Energy. *Nat. Mater.* **2009,** *8*, 837–842.
10. Hong, R.; Han, G.; Fernandez, J. M.; Kim, B.; Forbes, N. S.; Rotello, V. M. Glutathione-Mediated Delivery and Release Using Monolayer Protected Nanoparticle Carriers. *J. Am. Chem. Soc.* **2006,** *128*, 1078–1079.
11. Berciaud, S.; Cognet, L.; Blab, G. A.; Lounis, B Photothermal Heterodyne Imaging of Individual Non-fluorescent Nanoobjects. *Phys. Rev. Lett.* **2004,** *93*, 257402.
12. Kang, S. Y.; Kim, K. Comparative Study of Dodecanethiol-Derivatized Silver Nanoparticles Prepared in One-Phase and Two-Phase Systems. *Langmuir* **1998,** *14*, 226–230.
13. Berciaud, S.; Lasne, D; Blab, G. A.; Cognet, L.; Lounis, B. Photothermal Heterodyne Imaging of Individual Metallic

Nanoparticles: Theory *versus* Experiment. *Phys.Rev. B* **2006,** *73*, 045424.
14. Sée, V.; Free, P.; Cesbron, Y.; Nativo, P.; Shaheen, U.; Rigden, D. J.; Spiller, D. G.; Fernig, D. G.; White, M. R. H.; Prior, I. A.; Brust, M.; Lounis, B.; Lévy, R.; Cathepsin, L Digestion of Nanobioconjugates upon Endocytosis. *ACS Nano* **2009,** *3*, 2461–2468.
15. Lasne, D.; Blab, G. A.; De Giorgi, F.; Ichas, F.; Lounis, B.; Cognet, L. Label-free Optical Imaging of Mitochondria in Live Cells. *Optics Express* **2007,** *15*, 14184–14193.
16. Alberts, B.; Johnson, A.; Lewis, J.; Raff, M.; Roberts, K.; Walter, P. The Cytoskeleton. In *Molecular Cell Biology of the Cell*, 4th ed.; Garland Science: New York, 2002, 907−929.
17. Octeau, V.; Cognet, L.; Duchesne, L.; Lasne, D.; Schaeffer, N.; Fernig, D. G.; Lounis, B. Photothermal Absorption Correlation Spectroscopy. *ACS Nano* **2009,** *3*, 345–350.
18. Luby-Phelps, K.; Mujumdar, S.; Mujumandar, R. B.; Ernst, L. A.; Galbraith, W.; Waggoner, A. S. A Novel Fluorescence Ratiometric Method Confirms the Low Solvent Viscosity of the Cytoplasm. *Biophys. J.* **1993,** *65*, 236–242.
19. Fushimi, K.; Verkman, A. S. Low Viscosity in the Aqueous Domain of Cell Cytoplasm Measured by Picosecond Polarization Microfluorimetry. *J. Cell. Biol.* **1991,** *112*, 719–725.
20. Yum, K.; Na, S.; Xiang, Y.; Wang, N.; Yu, M.-F. Mechanochemical Delivery and Dynamic Tracking of Fluorescent Quantum Dots in the Cytoplasm and Nucleus of Living Cells. *Nano Lett.* **2009,** *9*, 2193–2198.
21. Kuimova, M. K.; Yahioglu, G.; Levitt, J. A.; Suhling, K. Molecular Rotor Measures Viscosity of Live Cells *via* Fluorescence Lifetime Imaging. *J. Am. Chem. Soc.* **2008,** *130*, 6672–6673.
22. Swaminathan, R.; Bicknese, S.; Periasamy, N.; Verkman, A. S. Cytoplasmic Viscosity Near the Cell Plasma Membrane: Translational Diffusion of a Small Fluorescent Solute Measured by Total Internal Reflection-Fluorescence Photobleaching Recovery. *Biophys. J.* **1996,** *71*, 1140–1151.
23. Köhler, R.; Schwille, P.; Webb, W. W.; Hanson, M. R. Active Protein Transport through Plastid Tubules: Velocity Quantified by Fluorescence Correlation Spectroscopy. *J. Cell. Sci.* **2000,** *113*, 3921–3930.